JACS
JOURNAL OF THE AMERICAN CHEMICAL SOCIETY
Article
pubs.acs.org/JACS

Nitrite Reduction Mediated by Heme Models. Routes to NO and HNO?

Julie L. Heinecke,[†] Chosu Khin,[†] Jose Clayston Melo Pereira,[†] Sebastián A. Suárez,[‡] Alexei V. Iretskii,[†,§] Fabio Doctorovich,[‡] and Peter C. Ford*[,†]

[†]Department of Chemistry and Biochemistry, University of California at Santa Barbara, Santa Barbara, California 93106-9510, United States

[‡]Departamento de Química Inorgánica, Analítica y Química Física/INQUIMAE, Facultad de Ciencias Exactas y Naturales, Universidad de Buenos Aires, Ciudad Universitaria, Pabellon II, C1428EHA Buenos Aires, Argentina

[§]Department of Chemistry, Lake Superior State University, Sault Ste Marie, Michigan 49783, United States

Supporting Information

ABSTRACT: The water-soluble ferriheme model Fe^{III}(TPPS) mediates oxygen atom transfer from inorganic nitrite to a water-soluble phosphine (tppts), dimethyl sulfide, and the biological thiols cysteine (CysSH) and glutathione (GSH). The products with the latter reductant are the respective sulfenic acids CysS(O)H and GS(O)H, although these reactive intermediates are rapidly trapped by reaction with excess thiol. The nitrosyl complex Fe^{II}(TPPS)(NO) is the dominant iron species while excess substrate is present. However, in slightly acidic media (pH ≈ 6), the system does not terminate at this very stable ferrous nitrosyl. Instead, it displays a matrix of redox transformations linking spontaneous regeneration of Fe^{III}(TPPS) to the formation of both N_2O and NO. Electrochemical sensor and trapping experiments demonstrate that HNO (nitroxyl) is formed, at least when tppts is the reductant. HNO is the likely predecessor of the N_2O. A key pathway to NO formation is nitrite reduction by Fe^{II}(TPPS), and the kinetics of this iron-mediated transformation are described. Given that inorganic nitrite has protective roles during ischemia/reperfusion (I/R) injury to organs, attributed in part to NO formation, and that HNO may also reduce net damage from I/R, the present studies are relevant to potential mechanisms of such nitrite protection.

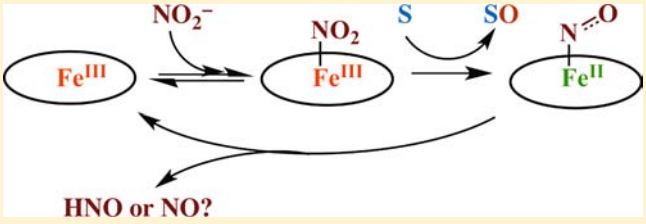

INTRODUCTION

Ionic nitrite has been shown to be protective of mammalian organs under ischemic physiology, and this activity has been attributed to nitrite (NO_2^-) conversion to nitric oxide, the latter being a regulator of hypoxic signaling responses.[1−5] For example, NO_2^- reduction to NO occurs in liver homogenates under conditions of low oxygen tension, and cytochrome P_{450} type proteins and thiols are reported to play major roles in this transformation.[6] Other ferrous heme proteins such as hemoglobin (Hb),[7,8] myoglobin (Mb),[9−11] neuroglobin,[12] and endothelial nitric oxide synthase (eNOS)[13] have been reported to act as nitrite reductases (NiRs) (eq 1, Fe(Por) = a heme protein or model).[14] Heme-mediated NiR activity is complicated by side reactions, specifically, the formation of stable ferrous heme nitrosyls (eq 2, $K_2 > 10^{11}$ M^{-1} for ferrous globins)[15−17] and NO dioxygenation by oxo-heme proteins (eq 3, $k_3 = 9 \times 10^7$ M^{-1} s^{-1} for $Hb(O_2)$).[18,19] Despite these complications, it has been shown that in isolated heart homogenates and red blood cells, nitrite reduction by Mb and Hb, respectively, generates sufficient NO to inhibit mitochondrial respiration.[20]

$$Fe^{II}(Por) + NO_2^- + 2H^+ \rightarrow Fe^{III}(Por) + NO + H_2O \quad (1)$$

$$Fe^{II}(Por) + NO \rightleftarrows Fe^{II}(Por)(NO) \quad (2)$$

$$Fe^{II}(Por)(O_2) + NO \rightarrow Fe^{III}(Por) + NO_3^- \quad (3)$$

Another pathway to NO formation from nitrite is by oxygen atom transfer (OAT) to substrates (S) as mediated by a metal center (eqs 4 and 5). Such transformations have been long known for metallo-phthalocyanines and -porphyrins in organic media[21−23] and more recently have been shown in solid matrices.[24,25] One such report described OAT from a mixture of Fe^{III}(OEP)Cl (OEP^{2-} = octaethylporphyrinato) and [K(18-crown-6)]NO_2 in *N*-methylpyrrolidone/acetic acid to various substrates while generating $Fe^{II}NO$.[23] However, this medium is strongly acidic, and acid-promoted nitrite disproportionation[26] forms NO_2 and N_2O_3, both being strong oxidants.[27] Thus, even in the absence of the Fe^{III}(OEP)Cl, analogous solutions of $NaNO_2$ in this medium still effect oxidations, for example, of PPh_3 to PPh_3O.[28]

$$ML_nX + NO_2^- \rightleftarrows ML_n(NO_2) + X^- \quad (4)$$

$$ML_n(NO_2) + S \rightarrow ML_n(NO) + SO \quad (5)$$

Received: December 17, 2012
Published: February 19, 2013

   dx.doi.org/10.1021/ja312092x | J. Am. Chem. Soc. 2013, 135, 4007−4017

More recently, we demonstrated similar Fe(III)-mediated OAT reactions from nitrite in aqueous solution (Scheme 1, step (a)). The Fe^{III}(Por) complexes were the ferriheme models Fe^{III}(TPPS) (**1**) or Fe^{III}(TMPS),[29] and the substrates (S) included a water-soluble phosphine (tppts), dimethyl sulfide (DMS), and the biological thiols cysteine (CysSH) and glutathione (GSH).[30,31] These reactions were carried out in pH 5.81 and pH 7.40 aqueous buffer solutions, where nitrite disproportionation is significantly less important than in more acidic media. The products were the corresponding substrate oxides and the respective ferrous nitrosyls Fe^{II}(Por)(NO) (eq 5). Furthermore, Fe^{II}(TPPS)(NO) (**2**) was found to undergo spontaneous regeneration to the ferric complex **1**. Thus, the ferrous nitrosyls, despite their well-known stability,[32] are not simply dead-end products. Instead, they are part of a dynamic catalytic system. Described here are studies directed toward defining these transformations and their mechanisms that serve as models for the analogous transformations in mammalian heme proteins.

Scheme 1. Catalytic Cycle Where (a) the Water-Soluble Fe^{III}(Por)(NO_2^-) Oxidizes Substrates To Form Fe^{II}(Por)(NO) and (b) Fe^{II}(Por)(NO) Spontaneously Regenerates Fe^{III}(Por) in the Absence of Oxygen[a]

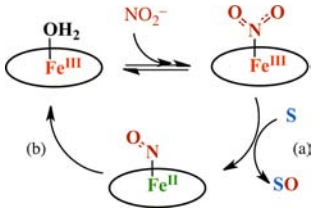

[a]The ovals represent the porphyrins. The proximal ligand is likely to be H_2O for the ferric species.

EXPERIMENTAL SECTION

Materials. Fe^{III}(TPPS) (**1**) and Fe^{III}(TMPS) (**3**) were purchased from Midcentury Chemicals, and tris(3-sulfonatophenyl)phosphine (tppts) was synthesized by T. L. Matson of this laboratory by a published procedure[33] and purified by passing through a G-25 Sephadex column. Sodium nitrite (99.999%) and the remaining chemicals were of the highest purity and purchased from Sigma-Aldrich. Angeli's salt ($Na_2[N_2O_3]$) was a gift from Prof. Jon Fukuto at Sonoma State University. Nitric oxide gas (99.5%) was purchased from Praxair and purified by passing through an Ascarite II filled stainless steel column submerged in dry ice/acetone bath (−78 °C)[34] to remove any adventitious NO_x. Nitrous oxide gas was purchased from Sigma-Aldrich and used without further purification for the standardization of GC and FTIR.

Solution Preparations. The rates of substrate oxidations by the $NaNO_2$/Fe^{III}(TPPS) system were studied in pH 5.81 buffered solutions (50 mM phosphate) at 25 °C under deaerated conditions unless otherwise noted. Reaction solutions for these studies were prepared in custom Schlenk line glassware equipped with a 1.0 cm path length quartz cell, a septa sealed electrode adaptor (Thermogreen LB2 from Sigma), and a small round-bottom flask (Supporting Information Figure S-1). Solutions were deaerated by freeze−pump−thaw techniques, then backfilled with high-grade argon (1 atm). Substrates were added to the $NaNO_2$/Fe^{III}(TPPS) system using argon purged gastight syringes, and changes in the optical spectra were used to monitor the reaction progress.

Solutions of the ferrous nitrosyl complex Fe^{II}(TPPS)(NO) (**2**) alone were generated by reductive nitrosylation of **1** by excess NO in pH 5.81 or pH 7.40 solution. The excess NO was then removed by freeze−pump−thaw techniques or by evacuating the flask at room temperature followed by backfilling with argon.

For nitrite reductase studies, the ferrous complex Fe^{II}(TPPS) was prepared by reduction of **1** with a slight excess of sodium dithionite (15 μM) in pH 5.81 buffered solution. The reaction was initiated once the dithionite (λ_{max} = 314 nm, $\varepsilon_{max} = 8 \times 10^3$ M^{-1} cm^{-1}) decomposed, as evidenced from the spectral changes. All substrate additions to solutions were effected using argon purged, gastight syringes via the septa sealed electrode adapters.

Reactions of tppts with HNO generated by the decomposition of Angeli's salt (AS) were studied in pH 5.81 and pH 7.40 phosphate buffered solutions with 10% D_2O. Solid AS was added to a J-Young NMR tube to which a gas sampling, septa sealed electrode adapter could be attached. The NMR tube was purged with argon, and 0.6 mL of a degassed tppts solution was added after which the ^{31}P NMR spectrum was monitored (see below). Once the reaction was complete, headspace aliquots were removed and analyzed for N_2O.

The kinetics of the reaction between aqueous tppts and NO were studied under deaerated conditions using the Schlenk type cell illustrated in Supporting Information Figure S-1. A solution (3.0 mL) of tppts (0.56 mM) in pH 5.81 solution (50 mM phosphate) was introduced to the cell and then deaerated by freeze−pump−thaw techniques. Gaseous NO was either added directly to the cell measured by the manometer and pressurized to 1 atm of Ar or the cell was pressurized to 1 atm Ar and known volumes of NO were added to the cell using gastight syringes, and spectral changes were monitored by recording the optical spectrum every 20 s. Between the spectral measurements, the reaction flask was vigorously shaken to maintain the equilibrium between the liquid and gas phases. Because the solubility of NO in aqueous solution is relatively low and the volume of the gas phase (28 mL) was much larger than that of the solution phase (3.0 mL), the total amount of NO present in the system (100−250 μmol) was in substantial excess of the tppts present (1.7 μmol), so that the solution-phase NO concentration remained at a near constant value (pseudo first-order conditions) throughout any one study.

Instrumental Methods. Optical absorbance measurements were recorded using a Shimadzu dual beam UV-2401 PC spectrophotometer in 1.00 cm path-length quartz cells and referenced to the respective buffer solutions. For all kinetics studies, the spectrometer cell compartment was thermostatted to 298 K. The $^{31}P\{^1H\}$ NMR spectra were recorded on a Bruker DMX-500 NMR spectrometer at 202.45 MHz for ^{31}P and 500.13 MHz for ^1H with a 2 s time delay. Phosphorus chemical shifts were referenced to 85% H_3PO_4, and the spectra were processed using TopSpin software. The ESI−MS^+ of the reaction products was analyzed using a Waters Micromass Q-TOF-2 mass spectrometer.

Infrared spectra (400−4000 cm^{-1}) with 1 cm^{-1} resolution were recorded with a research series FT Mattson FTIR spectrophotometer. All gas-phase IR spectra were recorded using an 8 cm path length gas cell with CaF_2 windows. The reaction vessel was equilibrated with the IR cell under reduced pressure using a t-joint, and then the cell was backfilled with argon to ∼1 atm to minimize pressure effects on the extinction coefficient. The IR spectrum of the N_2O present was quantified using calibration curves for the absorption at 2212 and 2236 cm^{-1} for the P and R branches, respectively. The detection limit for this system was 0.2 μmol of N_2O. Alternatively, the gas phase above the reacting system was sampled using a gastight syringe and was analyzed by gas chromatography using an Agilent Technologies model 6890 GC and a 30 m Carbosieve packed column with a 300 °C max temperature. The GC was operated with the inlet and detector at 250 °C with the following temperature program: Initial T was 125 °C for 5 min, then T was ramped at 40 °C/min to 240 °C and held for 10 min. The carrier gas was helium at a constant flow at 31.46 psi (gauge), and the software used was GC ChemStation Rev.B.01.03[204]. Under these conditions, nitrous oxide had a retention time (R_T) of 11.3 min, and N_2O signals for each injection were compared to a calibration curve prepared by injecting samples of pure N_2O. The detection limit was 2 nmol. The concentrations of NO and N_2O in the reaction solutions were determined from the composition of the injection samples, the volumes of the injection sample, the reaction cell, and the

dx.doi.org/10.1021/ja312092x | J. Am. Chem. Soc. 2013, 135, 4007−4017

solution, and the partition coefficients for NO (20.9)[35] and N_2O (1.65)[36] between the gas and aqueous phases.

Nitric oxide was detected and analyzed using a GE Sievers model 280i nitric oxide analyzer (NOA). Known volumes of the gases from the solution headspace were injected into the NOA purge vessel, and these gases were entrained to the detector using helium. The NO present in the sample was quantified using a calibration curve generated from the reaction of $NaNO_2$ with acidic KI.

Amperometric analysis for HNO formation was carried out as described previously[37] with a TEQ 03 potentiostat and a three-electrode system consisting of platinum counter electrode, a Ag/AgCl reference electrode, and a gold working electrode modified with a monolayer of cobalt porphyrin with 1-decanethiol covalently attached. This modified electrode has been demonstrated to be specific for HNO,[37] as NO, nitrate, nitrite, and Fe^{II}(TPPS)(NO) showed no current. The release of HNO from AS was used to calibrate this analysis, and the reactions considered for HNO detection by the electrode are shown in Scheme S-1. Modeling of the electrode current was achieved by numerical integration of a set of differential equations representing the mechanism of the reactions involved as well as those taking place at the electrode surface; the reactions, rate laws, and rate constants are shown in Table S-1. The SimBiology toolbox from Matlab 2009b was used to solve the equations and fit the current.

DFT calculations for iron containing species were performed at unrestricted TPSSTPSS/DGDZTVP level of theory in the gas phase using the Gaussian 03 software package. In limited cases, a solution-phase geometry optimization using a polarized continuum medium (PCM) was completed to assess the influence of a solvent (water).

RESULTS AND DISCUSSION

A. Fe(TPPS)-Mediated Oxygen Atom Transfer from Nitrite to Various Substrates. *Substrate Oxidation and the Formation of Nitrosyl Complexes.* Two communications from this laboratory[30,31] have described the reaction of aqueous Fe^{III}(TPPS) (**1**) and sodium nitrite with various substrates (S) to give Fe^{II}(TPPS)(NO) (**2**) and oxidized substrate (SO) and will be briefly summarized and expanded upon here. Figure 1 illustrates the temporal spectrum changes after addition of the water-soluble phosphine tppts (1 mM) to solutions containing **1** (8 μM) and $NaNO_2$ (10 mM) at pH 5.81 (50 mM phosphate buffer). The transformation of **1** (λ_{max} 393 and 528 nm) to **2** (λ_{max} 413 and 543 nm) was indicated by shifts in the characteristic Soret and Q bands of the optical spectra for these very strongly absorbing chromophores. Distinct isosbestic points at 403, 489, 540, and 615 nm were also observed. The rate of absorbance change did not follow a simple exponential (Figure 1, inset); therefore, the initial rate method was used to probe the kinetics dependence on reactant concentrations. From these data, the rate law was determined to be first order in $[NO_2^-]$, first order in [**1**], and first order in [tppts] (eq 6) with a rate constant k_{OAT} of 2.1×10^2 M^{-2} s^{-1}.[28] This behavior is consistent with the reversible formation of the ferric nitrite complex Fe^{III}(TPPS)(NO_2^-) (K = 3 M^{-1})[38] followed by rate-limiting reaction with the substrate (k_2 = 70 M^{-1} s^{-1}) to form **2** plus the phosphine oxide tpptsO as depicted in Scheme 1.

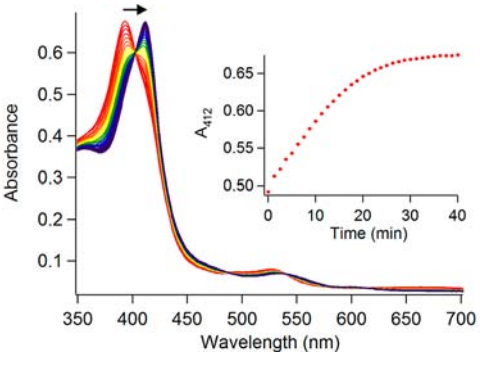

Figure 1. Spectral changes and kinetic trace (inset) for the reaction of Fe^{III}(TPPS) (**1**, 8 μM) and $NaNO_2$ (10 mM) with tppts (1 mM) in pH 5.81 aqueous solution. The spectrum changes directly from that of **1** (λ_{max} 393 nm, ε_{max} = 1.6×10^5 M^{-1} cm^{-1}) to that of Fe^{II}(TPPS)(NO) (**2**, λ_{max} 413 nm, 1.55×10^5 M^{-1} cm^{-1}) with no apparent intermediates. The reaction is nearly complete within 30 min (inset).

$$-(d[\mathbf{1}]/dt) = k_{OAT}[NO_2^-][\mathbf{1}][tppts] \quad (6)$$

After the formation of **2** was complete, the tpptsO was identified by in situ ^{31}P NMR and by mass spectroscopy. The phosphine oxide was not formed in significant quantities in analogous solutions that were prepared from $NaNO_2$ and tppts but did not contain **1** even after 1 week. Such OAT from a nitrite complex of a ferriheme is consistent with earlier computational studies that indicate the feasibility of this reaction.[39]

Similarly, we showed that when dimethyl sulfide (DMS) was the substrate, the product was dimethylsulfoxide as identified by GCMS techniques, but DMSO was not formed in the absence of **1**. These solution-phase experiments parallel studies in porous layered solids by Kurtikyan et al.[25] that demonstrated ^{18}O transfer from the 6-coordinate *N*-nitrito complexes Fe^{III}(TPP)(L)($N^{18}O_2$)[29] to the sulfides DMS and tetrahydrothiophene (THT) to give the respective ^{18}O labeled sulfoxides with concomitant formation of Fe(TPP)(L)($N^{18}O$) (L = DMS or THT).

The ferrous nitrosyl product **2** was also observed when cysteine or glutathione were the substrates in pH 5.81 aqueous solutions of **1** (8 μM) and $NaNO_2$ (10 mM). Notably, the organic products were the respective disulfides cystine or GSSG as identified by mass spectrometry.[30] However, trapping studies using dimedone, which is specific for sulfenic acids, demonstrated that the OAT products, the sulfenic acids RS(O)H, are formed as intermediates (see below). The kinetics of CysSH oxidation were further complicated by the rapid formation of the ferric thiolate, Fe^{III}(TPPS)($CysS^-$), in a dead-end equilibrium (eq 7, K_7 = 230 ± 50 M^{-1}, pK_a = 4.7 ± 0.1).[31] Nonetheless, the rate of the slow formation of **2** proved to be first order in [$NaNO_2$] and in [**1**] and approached first order in [CysSH] at low thiol concentrations.[31]

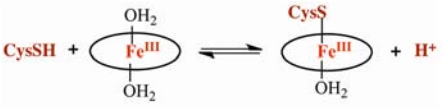

(7)

The analogous reaction of CysSH was also studied using a different water-soluble ferric porphyrin complex, Fe^{III}(TMPS) (**3**), which has bulky mesityl groups at the porphyrin meso positions that inhibit formation of μ-oxo Fe^{III}–O–Fe^{III} dimers at higher pH (a major complication for studies with **1**). At pH 5.81, the reaction of **3** with CysSH and nitrite to give Fe^{II}(TMPS)(NO) (**4**) behaved quite similarly to the reaction of **1** under analogous conditions. There was a fast initial absorbance change due to formation of the cysteinate complex as in eq 7, followed by slower reaction with nitrite to give the ferrous nitrosyl as characterized by its broad Soret band at 407

dx.doi.org/10.1021/ja312092x | J. Am. Chem. Soc. 2013, 135, 4007–4017

nm and Q bands at 477 and 539 nm. In buffered solutions at pH 7.4, CysSH addition to a solution of **3** led to a similar initial spectral shift followed by formation of **4**. The temporal changes indicated that formation of **4** was slower at the higher pH due to the increased importance of the dead-end equilibria forming Fe^{III}(TMPS)($CysS^-$) and the hydroxo complex Fe^{III}(TMPS)-(H_2O)(OH)[31] (see Supporting Information Scheme S-2).

Sulfenic Acid Products from CysSH and GSH. As noted above, oxygen atom transfer to CysSH or GSH from the mixture of NO_2^- and the ferri-heme model **1** would have been expected to generate initially the respective sulfenic acid derivatives CysS(O)H and GS(O)H. However, mass spectral studies of the product solutions showed instead the presence of the corresponding disulfides cystine and GSSG. This can be explained in terms of trapping of any sulfenic acid formed by the excess thiols (~1 mM) to give disulfides (Scheme 2).[40] Thus, we employed dimedone (**D**) as a competitive trapping agent to probe the potential intermediacy of sulfenic acid OAT products.[31]

Scheme 2. Heme-Mediated OAT to RSH (CysSH or GSH) Gives the Sulfenic Acid, RS(O)H, Which Is Trapped by Excess RSH To Form RSSR or by Dimedone (D) To Give D−SR

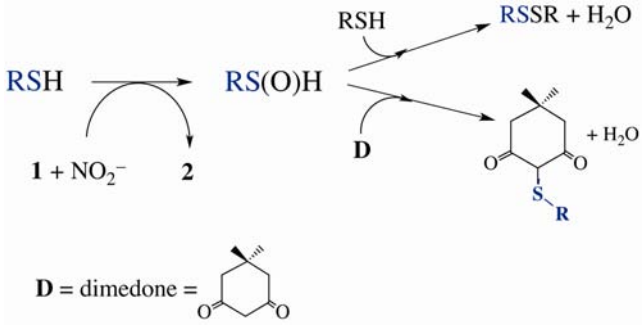

Dimedone is a specific trapping agent for RS(O)H,[41] and the product is the corresponding thiol ether (Scheme 2) that can be identified by LC/MS techniques. For example, when **D** (1 mM) was added to a deaerated, pH 5.81 aqueous solution of **1** (8.6 μM) and $NaNO_2$ (10 mM) just before RSH addition (1 mM, either CysSH or GSH), the reaction proceeded to form the ferrous nitrosyl **2**, according to the changes in the optical spectrum. The respective cysteine and glutathione thioethers expected from dimedone trapping of RS(O)H intermediates were detected and identified by LC/MS analysis of the product solutions. The analogous products were similarly identified for the reaction at pH 7.4 using the TMPS complex **3** (8.6 μM), $NaNO_2$ (10 mM), RSH (1 mM), and **D** (1 mM) with either CysSH or GSH.

Notably, these thioether products were found only when a Fe^{III}(Por) was present. Furthermore, the addition of higher concentrations of CysSH or GSH led to smaller yields of the dimedone thioether adducts, and addition of a higher concentration of **D** led to an increase in the respective thioether.[31] Both of these observations are consistent with the competitive trapping of RS(O)H by RSH or **D** as illustrated in Scheme 2. Thus, we conclude that sulfenic acid intermediates are the initial products formed by OAT to CysSH and GSH as implied by step (a) of Scheme 1.

B. The Back Reaction: Nitrous Oxide Formation and Nitrite Reductase Activity. *Spontaneous Regeneration of Fe^{III}(TPPS) (1).* Notably, the ferrous nitrosyl product Fe^{II}(TPPS)(NO) (**2**) is not indefinitely stable after formation in the medium where the OAT reaction occurs. Regardless of the substrate, the introduction of traces of air led to changes in the spectrum indicative of the reformation of **1** and other products that were not investigated further. More surprisingly, even when dioxygen was rigorously excluded from the reaction vessel, slow regeneration of **1** (Soret band λ_{max} 393 nm) and disappearance of **2** (λ_{max} 413 nm), step (b) of Scheme 1, were consistently observed (Supporting Information Figure S-2). Furthermore, this transformation proved to be faster at pH 5.81 than at higher pH and was accompanied by the formation of nitrous oxide when tppts was the substrate but not when CysSH was present.[30] In the context of this limited information, several potential mechanisms were suggested. The studies described below are largely focused on elucidating the pathways responsible for depletion of **2** and regeneration of **1**.

Figure 2 illustrates the temporal changes in the absorbance at 413 nm corresponding to the Soret band λ_{max} characteristic of **2**

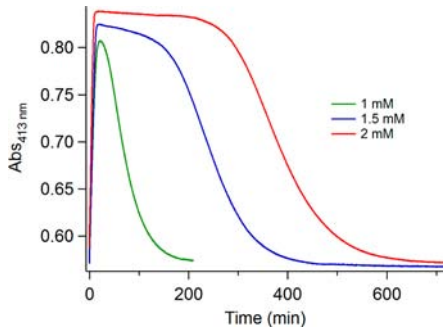

Figure 2. The temporal changes for the OAT reaction at pH 5.81 with Fe^{III}(TPPS) (**1**, 8 μM), $NaNO_2$ (10 mM), and several tppts concentrations (1−2 mM), showing fast initial formation of Fe^{II}(TPPS)(NO) (**2**, 413 nm) followed by slow reformation of **1**.

after mixing solutions of **1**, $NaNO_2$ (10 mM), and several concentrations of tppts at pH 5.81 (1.0, 1.5, and 2.0 mM). The initial fast formation of **2** was followed by a period where there was a roughly steady-state concentration of this product, followed by slow decay back to the spectrum of **1**. Similar behavior was seen when CysSH was the substrate (Supporting Information, Figure S-3); however, the regeneration time was considerably longer. After **1** was fully reformed, presumably as the result of substrate exhaustion, further addition of either tppts or CysSH led again to formation of **2** followed by slow decay back to the initial spectrum, indicating that the system remained active for OAT. Thus, under these conditions, the rate-limiting step(s) of the catalytic cycle indicated by Scheme 1 is the regeneration of **1** from **2**. When analogous reactions were carried out at higher pH, the rate of Fe^{III}(TPPS) reformation decreased (see below), and at pH 7.4 the rate was too slow to measure.

To provide a more quantitative estimate of rates, we have measured the time that the various reaction systems required to return from the maximum absorbance due to **2** found upon the OAT reaction initiated by mixing **1**, nitrite, and substrate to the absorbance where the concentrations of **2** and **1** were equal. This value that is defined here as $\tau_{r/2}$ is affected by the nature and concentration of the substrate as well as by the pH (Table 1). As expected, $\tau_{r/2}$ becomes longer when there is more

dx.doi.org/10.1021/ja312092x | J. Am. Chem. Soc. 2013, 135, 4007−4017

Table 1. Effect of Substrate Concentration and of pH on $\tau_{r/2}$[a]

[tppts][b] (mM)	1.0	1.5	2.0
$\tau_{r/2}$ (min)	71	240	376
pH[c]	5.65	5.81	6.25
$\tau_{r/2}$ (min)	81	240	570

[a] $\tau_{r/2}$ is the time required for a solution prepared from Fe^{III}(TPPS) (**1**, 10 μM), nitrite (10 mM), and the phosphine tppts (at 298 K) to return from the maximum concentration of Fe^{II}(TPPS)(NO) (**2**) first formed to the state where [**2**] = [**1**]. [b] pH 5.81. [c] [tppts] = 1.5 mM.

substrate to consume; however, the nonlinear relationship between the values of $\tau_{r/2}$ and [tppts] suggests that the time required for the system to cycle fully may be affected by feedback mechanisms. For example, we have shown previously that the OAT reaction to tppts is inhibited by the tpptsO product, presumably due to competitive binding of this species and NO_2^- to **1**.[28] The other feature of the data in Table 1 is the strong relationship between $\tau_{r/2}$ and pH that clearly shows that the catalytic cycle leading to full consumption of the substrate, and the concomitant return of the iron complex to **1** is faster in a more acidic medium.

Nitrous Oxide as a Product. In our earlier study, FTIR analyses of the headspace gases present after mixtures of **1**, nitrite, and tppts had reacted to full substrate exhaustion in pH 5.81 buffer solution clearly indicated that nitrous oxide is also a product of this system.[30] This technique showed that N_2O was formed when tppts was the substrate, but when CysSH was the substrate N_2O was not detected. In that study, we reported that the amount of N_2O generated corresponded to ~one-half the moles of tppts consumed, that is, approximately stoichiometric quantities in terms of substrate redox equivalents. However, the revised data described below suggest that this result was in error apparently due to a failure to appreciate the dramatic pressure dependence of the extinction coefficients of IR absorbances in the spectra of gas phase molecules.[42] The present data show that substantial quantities of nitrous oxide are indeed formed, but these are less than stoichiometric with substrate consumed.

Quantification of N_2O production was readdressed using a combination of FTIR and GC analysis. For example, the reaction of **1** (8 μM), nitrite (10 mM), and tppts (1.0 mM) was run in a Schlenk-type cell of the type illustrated in Supporting Information Figure S-1. The 3.0 mL solution contained initially 0.024, 30, and 3.0 μmol of the respective reactants. After spectral changes indicated the complete regeneration of **1**, the reaction cell was equilibrated with an 8 cm path length CaF_2 IR cell connected by t-joint. The IR cell was then pressurized to ~1 atm with argon and the FTIR spectrum was recorded, the gas-phase N_2O spectrum showing the characteristic P and R branches (Supporting Information Figure S-4). The amount of N_2O present was then calculated by comparison to an IR absorbance calibration curve generated by recording the FTIR spectra of gas mixtures containing different amounts of pure N_2O pressurized to ~1 atm with argon. From this measurement together with the respective gas and liquid volumes and the partition coefficient between the liquid and gas phases (see Experimental Section), the quantity of N_2O formed was calculated as 0.42 μmol. GC analysis of a 500 μL aliquot of the gas phase gave a similar, but somewhat larger, quantity of N_2O (0.69 μmol) generated by the same reaction system. The latter value is considered the more reliable given the pressure sensitivity of the FTIR measurement and the need to repressurize the cell before recording the spectrum. Thus, while the N_2O formed proved to be considerably greater than the quantity of **1** initially present, the yield was only about one-half (46%) the amount predicted (1.5 μmol), if the oxidation of tppts to tpptsO were entirely due to the heme-mediated reduction of NO_2^- to N_2O. Notably, within detection limits, no N_2O was formed after 12 h by a control solution containing $NaNO_2$ (10 mM) and tppts (1 mM) but not containing Fe(TPPS) complexes (Supporting Information Figure S-4).

The pH effect on Fe^{III}(TPPS) reformation and the observation of N_2O as a product led to our proposal[30] that HNO was slowly generated via the protonation of **2** to form a nitroxyl complex (Scheme 3). Dissociation of HNO would give

Scheme 3. Proposed Formation of HNO

$$Fe^{II}(TPPS)(NO) + H^+ \rightleftharpoons Fe^{III}(TPPS)(HNO) \rightleftharpoons Fe^{III}(TPPS) + HNO$$

$$2HNO \longrightarrow H_2O + N_2O$$

1, while rapid dehydrative dimerization of HNO would form N_2O.[43] The absence of N_2O in the CysSH reaction is consistent with this hypothesis, because it is well-known that HNO is trapped by thiols to give sulfinamides.[44−47]

Analysis for HNO Formation. There are other potential pathways to nitrous oxide, so alternative tests for HNO generation are necessary to evaluate the pathway suggested by Scheme 3. For example, in an earlier study, Reisz et al.[48] reported that tris(4,6-dimethyl-3-sulfonato-phenyl)phosphine (trisodium salt) reacts with HNO in pH 7.4 aqueous solution to form a 1:1 ratio of the phosphine oxide (R_3PO) and aza-ylide ($R_3P(NH)$) (eq 8), the formation of which can be evaluated by ^{31}P NMR. The respective chemical shift values for R_3PO and $R_3P(NH)$ of this phosphine are 39.8 and 34.5 ppm versus phosphoric acid in buffered aqueous solution, and nitrite did not interfere with their analysis. Analogous reactivity should be observed with the analogous water-soluble phosphine tppts, and this supposition was tested by examining the products from the reaction of equimolar (0.5 mmol) tppts and the HNO donor AS in pH 5.81 solution (0.6 mL of buffer containing 10% D_2O) for 30 min. The ^{31}P NMR spectrum of the resulting solution indicated the depletion of the signal for tppts (−5.0 ppm vs phosphoric acid) and the formation of tpptsO (34.5 ppm) and another species (35.5 ppm) consistent with formation of tppts(NH) in a roughly 1:1 ratio (Supporting Information Figure S-5). The latter species was relatively stable, although the ^{31}P NMR spectra did show it to hydrolyze to tpptsO over a period of 36 h (data not shown). Consistent with tpptsO and tppts(NH) being formed by the trapping of HNO by tppts, GC analysis of the head space from such solutions showed only ~15% of the N_2O seen for the analogous decay of AS in the absence of tppts.

$$2R_3P + HNO \rightarrow R_3PO + R_3P(NH) \quad (8)$$

In this context, it is notable that the ^{31}P NMR spectrum of the products recorded 12 h after preparing a deaerated, ambient temperature solution of **1** (8 μM), NO_2^- (10 mM), and tppts (1 mM) showed not only the resonance for tpptsO at 34.5 ppm but also one at 35.5 ppm consistent with formation of tppts(NH) (Supporting Information Figure S-6), at about one-third of the intensity of the phosphine oxide. The lower but significant intensity of the latter signal would be expected

dx.doi.org/10.1021/ja312092x | J. Am. Chem. Soc. 2013, 135, 4007−4017

because tpptsO is also the product of the OAT reaction (see above). While this observation would be consistent with the HNO hypothesis, the pH of our experiment (5.81) was lower than that (7.4) used by Reisz et al.[48] As a control, nitrite (10 mM) was allowed to react with tppts (1 mM) in pH 5.81 solutions for 12 h. Surprisingly, the ^{31}P NMR spectrum of the product solution revealed resonances at 34.5 and 35.5 ppm (Figure S-7). Previously, we reported that the ^{31}P NMR did not show significant formation of the tppts oxide after 1 week, and no peak at 35.5 was identified. These solutions were measured after a prolonged reaction time, and any aza-ylide that may have been generated would have undergone hydrolysis to the oxide. If indeed the peak at 35.5 ppm after 12 h represents the aza-ylide, it is not clear how this might have formed, given that analogous solutions showed no N_2O production. Thus, the results of the trapping experiments with tppts appear to be ambiguous.

Another approach to HNO detection is the amperometric method recently developed by Suarez et al[37] using a gold electrode modified with Co(Por) (Por^{2-} = 5,10,15,20-tetrakis-[3-(*p*-acetyl-thiopropoxy)phenyl]porphyrinato) as a HNO specific sensor. The OAT reaction was carried out with this detector in deaerated pH 5.81 phosphate buffer solution using the following concentrations: **1** (8 μM), $NaNO_2$ (10 mM), and tppts (1.5 or 0.1 mM). Sodium nitrate (0.1 M) was added as supporting electrolyte to achieve good conductivity ($NaNO_3$ alone showed no detectable signal), and the electrochemical measurements were calibrated versus the release of HNO from different concentrations of Angeli's salt (AS) (Figure S-8). Upon adding tppts (1.5 mM) to a solution of Fe^{III}(TPPS) and nitrite, a strong positive signal for HNO was observed to rise slowly (Figure 3). A total of ~3 μmol of HNO was generated

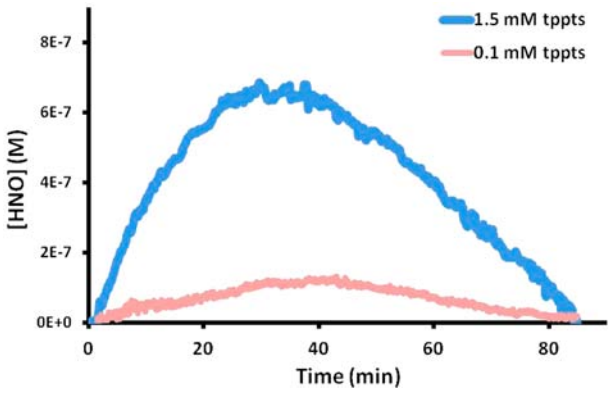

Figure 3. Temporal [HNO] detected using the cobalt-modified gold electrode[37] as generated by pH 5.81 buffered solutions containing Fe^{III}(TPPS) (**1**, 8 μM), $NaNO_2$ (10 mM), and tppts at 1.5 mM (blue) or 0.1 mM (pink). The supporting electrolyte was $NaNO_3$ (0.1 M). The plots are the average of two independent runs (see Figure S-9 for the individual raw data).

according to the AS calibration curve. This was approximately equivalent to the amount of HNO released by a 1 mM solution of AS under the same conditions. This would correspond to a ~67% yield of HNO based upon the reducing equivalents of the tppts added to the reaction solution. Given that under these conditions with the tppts concentration at 1.5 mM, ~3000 nanomol of HNO was detected in a solution containing only 24 nanomoles of **1**, HNO production is clearly catalytic in the iron species. Addition of less tppts (0.1 mM) produced much less HNO (Figure 3).

Notably, when **1** was not present, addition of tppts (1.5 mM) to an analogous solution of sodium nitrite (10 mM) led to the formation of trace amounts of HNO, but this was only ~5% of that produced in the presence of **1**. Thus, the amperometric technique clearly demonstrates that substantial HNO is formed in this reaction system in a process coupled to Fe^{III}(TPPS), nitrite, and tppts.

If all of the HNO detected in the OAT reaction of the 1.5 mM tppts solution were to dimerize, the resulting amount of N_2O would have been 1.5 μmol. For comparison, the GC experiments quantifying the nitrous oxide formed by a solution initially 1.0 mM in tppts (see above) gave a N_2O yield of 0.69 μmol (46% of the theoretical maximum), a yield that is of a magnitude similar to that (67%) for the HNO detected directly. Furthermore, as we have noted, the phosphine itself can act as a trap for HNO, although it is less efficient than are the thiols. Any such trapping would serve both to diminish the net yield of N_2O and to deplete the tppts substrate. Similarly, NO is known to trap HNO (second-order rate constant = 5.8×10^6 M^{-1} s^{-1}),[49] and as noted below, NO is also generated during the Fe(TPPS)-mediated nitrite oxidation of tppts.

The observation that HNO is indeed generated, albeit to a much lesser extent, in the solutions containing only nitrite and tppts may explain the ^{31}P NMR results noted above. The dimerization to give nitrous oxide would be second order in HNO, while the trapping of this reactive species by excess phosphine would be first order. As a consequence, the slower production of HNO in the uncatalyzed system would be expected to result in more efficient trapping by tppts to give the oxo- and aza-phosphine and much less N_2O.

If HNO were indeed produced according to Scheme 3, one would expect to observe the signature N_2O product from the spontaneous reactions of **2** in the absence of the other reaction components. Accordingly, **2** was generated in the absence of added NO_2^- by the (slow) reductive nitrosylation of **1** (10 μM) under excess NO at pH 5.81.[38] The excess NO was removed, and the reaction cell was backfilled with argon. After NO removal, the spontaneous back reaction of **2** proceeded over 5 h at ambient temperature to reform **1**, and this occurred both in the absence and in the presence of added tppts (1 mM). Thus, tppts does not reduce **1** in the absence of nitrite. There was no measurable formation of N_2O detected in GC-TD traces recorded for 500 μL aliquots of the headspace gas (data not shown, estimated detection limit is 2 nmol). However, it should be noted that the maximum amount of N_2O anticipated by this experiment in 3 mL solution would be only 15 nmol. In a related experiment, **2** was similarly generated but remained under NO (1 atm) for a period of 36 h. Under these conditions, the spectrum remained that of **2**. Samples of the headspace were analyzed by gas chromatography after 0, 12, and 36 h. Again, nitrous oxide (above the small background) was not detected in either of the latter samples (data not shown). Thus, one can conclude that the N_2O product seen when both nitrite and tppts are present is not due to Fe(TPPS)-mediated disproportionation of NO. Furthermore, these results suggest that the formation of HNO from **2** in these reactions systems must also involve the additional presence of nitrite or tppts in the solution.

NO Reduction by tppts? Although the nitric oxide initially formed by the OAT reaction would be strongly coordinated to the Fe^{II}(TPPS) moiety (Scheme 1), it is necessary to consider

the possibility of NO dissociation and reaction with the triarylphosphines according to eq 9:

$$R_3P + 2NO \xrightarrow{k_9} R_3PO + N_2O \quad (9)$$

because this is another possible pathway to N_2O formation. In an earlier study from this laboratory,[50] the reaction of triphenylphosphine with NO was shown to be first order in [Ph_3P] and second order in [NO], with third-order rate constants k_9 of 90, 1.05×10^3, and 1.57×10^3 M^{-2} s^{-1} in 294 K toluene, chloroform, and 1,2-dichloroethane, respectively. Substantial substituent effects were observed. However, phenyl ring sulfonates are but modestly electron withdrawing,[51] so major reactivity differences between Ph_3P and tppts in the analogous media would not be expected. The reaction was proposed to proceed through reversible formation of an intermediate with the composition $R_3P(N_2O_2)$ (K_P),[50] which would be stabilized by a more polar medium (Scheme 4),

Scheme 4. Proposed Pathway for NO Oxidation of Triarylphosphine by NO

$$R_3P + 2\,NO \underset{}{\overset{K_p}{\rightleftharpoons}} R_3P(N_2O_2) \xrightarrow{k_p} R_3PO + N_2O$$

where $k_9 = K_P k_P$. A subsequent DFT study (B3LYP/6-31+G*) of the model reaction of PH_3 + 2NO has concluded that $R_3P(N_2O_2)$ adduct is likely to be a 1,4-dioxoazaphosphole formed by coordinating both oxygens of the N_2O_2 dimer to the phosphine.[52] DFT calculations (B3LYP/6-311+G**) in this laboratory confirmed that a 1,4-dioxoazaphosphole intermediate provides the lowest energy in silico path to the products of eq 9 (R_3P = $^iPr_3P$, Supporting Information Figure S-10).

To evaluate the potential contribution of the NO/tppts reaction under the present conditions, the kinetics were investigated in pH 5.81 (50 mM phosphate buffer) solution by monitoring temporal absorbance changes at 290 nm, corresponding to the loss of tppts. The experiments were conducted in a Schlenk spectrophotometer cell (Supporting Information Figure S-1) for which the headspace volume (28 mL) greatly exceeded that of the solution (3.0 mL). Thus, the bulk (>99%) of the NO equivalents was in the headspace due to the gas/aqueous liquid partition coefficient (20.9),[35] and the solution [NO] was maintained at an approximately constant value by shaking the cell between spectral measurements. First-order kinetics were observed under these conditions. A plot of the resulting k_{obs} values versus $[NO]^2$, where [NO] is the calculated solution-phase nitric oxide concentration (0.14−0.44 mM), proved to be linear with a slope (k_9) of $(3.9 \pm 0.4) \times 10^4$ M^{-2} s^{-1} (Figure 4). This value is much larger than those determined in organic solvents in accord with the reaction being faster in more polar media.

Nonetheless, this kinetics result suggests that the direct reduction of NO by tppts (Scheme 4) would be too slow to contribute significantly to N_2O generation under conditions of the OAT reactions. To test this conclusion, control reactions between a low steady-state NO concentration of 500 nM and tppts (1 mM) were investigated. These did not generate appreciable amounts of N_2O over a 12 h period according to the IR method (where we estimate the threshold of N_2O

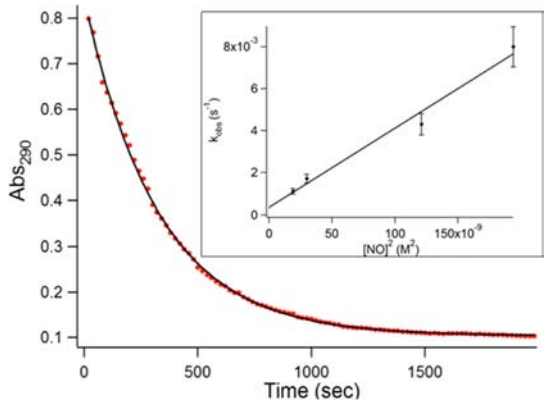

Figure 4. Temporal absorbance changes at 290 nm for the reaction of tppts (0.56 mM) with an approximately constant [NO] (0.14 mM, see text) fitted to a single exponential (k_{obs} of 1.3×10^{-3} s^{-1}). Inset: Plot for k_{obs} versus $[NO]^2$ giving $k_{11} = (3.9 \pm 0.4) \times 10^4$ M^{-2} s^{-1} (pH 5.81 at 298 K).

detection to be ∼200 nmol). When higher concentrations of both tppts (2 mM) and NO (2 μM) were used, sufficient N_2O (∼250 nmol) was formed after 20 h to be detected by the IR technique. However, these studies show that it is unlikely that NO reduction by tppts is a major contributor to the nitrous acid formation in the present system.[53,54]

Nitric Oxide Production. Two potential NO sources in this system are the OAT reaction (Scheme 1) and acid disproportionation of nitrite (eq 10). The NO formed by heme-mediated OAT to tppts would be strongly coordinated to a ferrous heme (the dissociation constant for **2** is $\sim 10^{-13}$ M in aqueous solution),[16] while NO formed by nitrite disproportionation would also be low at this pH (∼100 nM). A third potential NO source would be from nitrite reductase activity of the ferrous complex Fe^{II}(TPPS) (**5**), although it is anticipated that the concentration of free **5** would be very low, unless other components in the system affect the $Fe^{II}/Fe^{II}(NO)$ equilibrium. In this context, the Sievers nitric oxide analyzer was used to probe the temporal [NO] in pH 5.81 reaction solutions containing **1**, $NaNO_2$, and either tppts or CysSH.

$$\begin{aligned} 2H^+ + 2NO_2^- &\rightleftharpoons 2HNO_2 \\ &\rightleftharpoons H_2O + N_2O_3 \\ &\rightleftharpoons NO + NO_2 \end{aligned} \quad (10)$$

Cysteine does not react directly with NO under anaerobic conditions,[55] so any free NO formed in the heme-mediated nitrite oxidation of CysSH should not be depleted. To evaluate possible NO production in this case, a reaction solution was prepared from **1** (10 μM), sodium nitrite (10 mM), and CysSH (1 mM) at pH 5.81. The presence of **2** was monitored by the Soret band absorbance at 413 nm, while the NOA was used to determine the temporal [NO] in headspace aliquots taken periodically over 10 h at 298 K (Figure 5). An analogous experiment was also carried out using tppts (2 mM) as the substrate. For **2**, the patterns were analogous to those described above. When tppts was the substrate, there was a rapid rise in absorbance at 413 nm to a near steady-state value close to complete conversion of **1** to **2** for several hours, followed by a gradual decay back to an absorption spectrum close to that of **1**. When CysSH was the substrate, the steady-state stage was much longer, so that even at 10 h, the heme complexes were

dx.doi.org/10.1021/ja312092x | J. Am. Chem. Soc. 2013, 135, 4007−4017

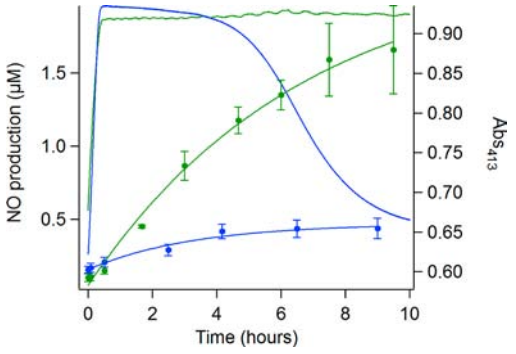

Figure 5. Reactions following addition of tppts (2.0 mM) or cysteine (1.0 mM), blue and green, respectively, to solutions of Fe^{III}(TPPS) (**1**, 10 μM) and nitrite (10 mM) monitored by using the NOA to determine the NO formation (dots) and by the temporal absorbance at 413 nm, the λ_{max} of Fe^{II}(TPPS)(NO) (**2**) (lines). The NO concentration in solution was calculated by determining that present in the gaseous head space and using the gas/aqueous solution partition coefficient to calculate $[NO]_{solution}$. (Note that a control reaction of tppts and nitrite without Fe(TPPS) did not lead to enhanced NO formation relative to nitrite solutions alone under the same conditions.)

mostly in the ferrous nitrosyl state. Furthermore, there was a marked difference in the ability of the two systems to generate NO. While $[NO]_{solution}$ was initially ~100 nM in both cases, NO generated from the tppts substrate leveled off at ~400 nM. For the CysSH substrate, this was ~4-fold higher at ~1.6 μM. Indeed, calculations using the relative volumes of the gas (28 mL) and solution (3.0 mL) phases in the reaction cell and the NO partition coefficient between the gas and aqueous phases indicate that total NO production from the respective reactions was ~235 nmol from the tppts (6 μmol total) and ~940 nmol from the CysSH (3 μmol total), even though in the latter case the system had not yet returned to the ferric state. The former value corresponds to a yield of ~2% of the theoretical maximum, if the sole reaction were the Fe(TPPS)-mediated reduction of nitrite to NO, while the latter corresponds to a ~16% yield. Therefore, free NO is also produced by the catalytic cycle, especially when cysteine is the reducing agent.

*Nitrite Reductase Activity of Fe^{II}(TPPS) (**5**).* It is clear that NO is produced by reactive systems containing nitrite, substrate, and Fe(TPPS) in molar quantities substantially exceeding that of the initially added **1** (typically 24–30 nmol).[56] While this result was especially apparent for the nitrite oxidation of CysSH (Figure 5), it was also true for tppts. What are the likely sources of this NO? Fe(TPPS) is clearly necessary for NO generation in both cases, hence it must be a catalyst, but if so, how can the ferrous complex participate in further nitrite reduction given the high stability of **2**?

To probe such questions, the nitrosyl complex **2** was generated in situ by the reductive nitrosylation of **1** (8 μM) in buffered solutions containing different concentrations of nitrite but no organic reductant.[38] After the excess NO was removed, the effect of nitrite concentration and of pH on the oxidation of **2** to **1** was probed by recording the time elapsed from initiation to when a 1:1 ratio of [**2**]:[**1**] was reached ($\tau_{r/2}$, described above). These data are summarized in Table 2 where it is obvious that increasing either $[H^+]$ or $[NO_2^-]$ in both cases accelerates the transformation of **2** to **1** in this medium.

Given that solutions of **2** spontaneously regenerate **1** at pH 5.81 when nitrite is present without added substrate, a plausible

Table 2. Effect of $[NO_2^-]$ and of pH on $\tau_{r/2}$[a]

$[NO_2^-]$[b] (mM)	2.0	5.0	10.0
$\tau_{r/2}$ (min)	491	319	145
pH[c]	5.81	6.05	6.25
$\tau_{r/2}$ (min)	145	300	430

[a] $\tau_{r/2}$ is the time required **2** (initially 8 μM) to evolve to a 1:1 ratio of **2** and **1** in the absence of other reductants at 298 K. [b] pH 5.81. [c] $[NO_2^-]$ = 10 mM.

explanation is that some ferrous complex in this medium reduces nitrite in analogy to the NiR activity of ferrous heme proteins.[7,9] This hypothesis was probed with solutions of Fe^{II}(TPPS) (**5**) prepared by the dithionite (~15 μM) reduction of **1** (10 μM) at various pH's (5.81–6.25). After the dithionite had spontaneously decayed,[57] $NaNO_2$ (6.6 mM) was added. The resulting temporal optical spectra showed a decrease of the Soret band for **5** (λ_{max} 412 nm) and appearance of a broad band consistent with a 1:1 mixture of **1** and **2** (Figure 6). Such

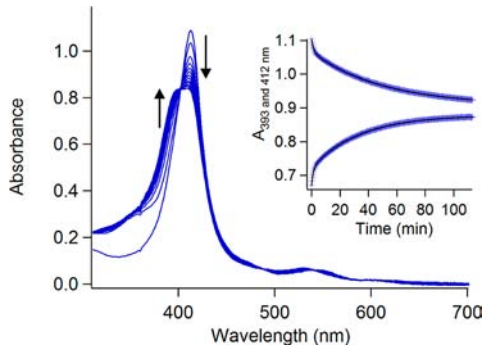

Figure 6. The reaction of Fe^{II}(TPPS) (**5**, 10 μM) and nitrite (6.6 mM) at pH 5.81 (50 mM phosphate) as monitored by the absorbance changes. The reaction proceeds from **5** (412 nm) to form a broad band due to the formation of a 1:1 ratio of Fe^{II}(TPPS)(NO) (**2**,413 nm) and Fe^{III}(TPPS) (**1**, 393 nm). Inset: Temporal absorption changes at 413 nm (above) and 393 nm.

behavior parallels the NiR activity demonstrated for ferro-heme proteins such as myoglobin,[9] where the NO generated rapidly traps an equivalent of **5** to give a 1:1 ratio of the ferro-heme nitrosyl and the ferri-heme (eq 11). The reaction depicted in eq 11 is quite favorable for Por = TPPS, in part due to the stability of the ferrous nitrosyl product. Although the reactions were not followed further in this case, the above results imply that this mixture will eventually evolve to a solution containing mostly **1**. The spectral changes display a fast initial phase followed by a slower one, so the initial rates method was used to evaluate the first stage. The response of the initial rates ($M\ s^{-1}$) to variations in the solution components indicated first-order behavior in $[NO_2^-]$ (3.3–13 mM) and in $[H^+]$ (eq 12, Supporting Information Figure S-11), consistent with eq 11. From these data, the second-order rate constant ($k' = k_{11}[H^+]$) for the reaction at pH 5.81 was calculated to be 0.024 ± 0.001 $M^{-1}\ s^{-1}$.

$$2Fe^{II}(Por) + NO_2^- + 2H^+ \rightleftharpoons Fe^{III}(Por) + Fe^{II}(Por)(NO) + H_2O \quad (11)$$

$$-d[\mathbf{5}]/dt = k_{11}[NO_2^-][H^+][\mathbf{5}] \quad (12)$$

A possible scenario for this NiR is shown in Scheme 5. The equilibrium and rate constants for spontaneous NO dissocia-

Scheme 5. Hypothetical Pathway for the Nitrite Reductase Reactions of Fe^{II}(TPPS) in Aqueous Solution[a]

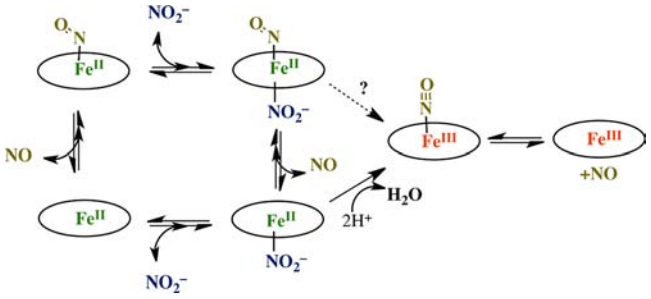

[a]Coordination sites without a ligand may be occupied by H_2O.

tion from **2** are both quite small ($K_d < 10^{-12}$ M, $k_{off} = 6.4 \times 10^{-4}$ s^{-1})[16] in aqueous solutions. Thus, it seems likely that NO dissociation may be promoted by association of **2** with a proximal ligand, most likely a nitrite ion. DFT studies, described briefly below, confirm the labilizing effect of a proximal *N*-nitrito ("nitro") group. Alternatively, the nitrosyl nitrito complex itself might react to give (transiently) a dinitrosyl iron(III) complex. The reaction kinetics briefly investigated do not differentiate these alternatives. Notably, the substrates in the OAT systems may also serve as trans labilizers of coordinated NO (see below), although as reported above, their presence is not a necessary condition for nitrite promoted transformation of **2** to **1**.

DFT computations of Fe^{II}(P)(L)(NO) (P = porphine dianion) were used to provide some insight into the potential significance of a proximal ligand L in labilizing nitric oxide from a ferro-heme nitrosyl. Various neutral and anionic ligands including H_2O, *O*- and *N*-coordinated nitrite ion, cysteine and cysteinate ion, dimethylsulfide, methylsulfide, and trimethylphosphine were considered. As noted previously,[58] the calculated Fe−NO bond distances and Fe−N−O angles of Fe^{II}(P)(L)(NO) are significantly affected by the proximal ligand. The former increases from ∼0.02 Å for L = H_2O, CysSH, and DMS to ∼0.08−0.09 Å for Me_3P, $CysS^-$, and *N*-nitrito relative to Fe^{II}(P)(NO) (see Supporting Information Figure S-12); the latter moves from a calculated angle of 144° for Fe^{II}(P)(NO) to 140° for L = H_2O and similar ligands to ∼138° for L = Me_3P, $CysS^-$, and *N*-nitrito. Interestingly, the largest calculated effects are seen for a proximal *N*-nitrito ligand, and these in silico results suggest that NO labilization may be promoted by nitrite coordination, and perhaps by coordination of the phosphine or thiol substrates. Furthermore, the more acute Fe−N−O angle of the proximal coordinated ferrous nitrosyl also invites the speculation that the NO is more negatively charged and therefore is more susceptible to protonation. Thus, coordination of nitrite (or a substrate such as a tppts or a thiolate) to **2** may also promote the formation of HNO as well as NO labilization (and subsequent nitrite reduction to a second NO). Both of these pathways lead to the formation of **1**, although it is important to note that both are acid dependent, thus activated by the lower pH's studied here. In the presence of excess nitrite, the OAT reaction closes the cycle back to **2** so long as a sulfide, thiol, or phosphine substrate is present. Thus, the heme is catalyzing the reduction of nitrite to NO and/or HNO by these substrates.

SUMMARY

We have described a complex matrix of transformations for an aqueous system composed of inorganic nitrite and reductants such as a water-soluble phosphine, dimethyl sulfide, or the biological thiols cysteine or glutathione and mediated by the heme-model Fe(TPPS). These processes include: (i) The ferric complex **1** promotes oxygen atom transfer from coordinated nitrite to the substrates tppts, DMS, CysSH, and GSH with concomitant formation of **2**. (ii) For the thiols CysSH and GSH, trapping studies show the initial products to be the respective sulfenic acids, functional groups that are drawing increasing attention with regard to their biological relevance as sensors of oxidative stress and in redox-based signaling.[59] (iii) The OAT product solutions do not terminate at the very stable ferrous nitrosyl **2**. Instead, spectral changes showing the slow regeneration of **1** are an indicator that the system remains dynamic with both N_2O and free NO being produced. (iv) Exploration of various pathways to nitrous oxide formation points to nitroxyl (HNO) as an intermediate product that undergoes dehydrative dimerization to give N_2O. The HNO intermediate was directly observed using a recently reported electrochemical HNO sensor.[37] (v) The nitrite reductase activity of the ferrous complex Fe^{II}(TPPS) is described, and it is suggested that the lability of ferrous nitrosyl complexes is enhanced by coordination of a nitrite ion or a thiol in the proximal site.

Furthermore, the production both of the transient HNO and of NO as the iron species cycles from **1** to **2** and back during the mediated oxidation of tppts by nitrite is clearly catalytic in Fe. Similar catalysis is evident in the iron-mediated oxidation of CysSH and the concomitant net production of NO

The overall reaction cycle proposed for the aqueous system composed of Fe^{III}(TPPS) (**3**), NO_2^-, and substrate (tppts, DMS, CysSH, or GSH) is illustrated by Scheme 6. Given the

Scheme 6. Compendium of Reactions Described for pH 5.81 Solutions of Fe(TPPS), Nitrite, and Various Substrates[a]

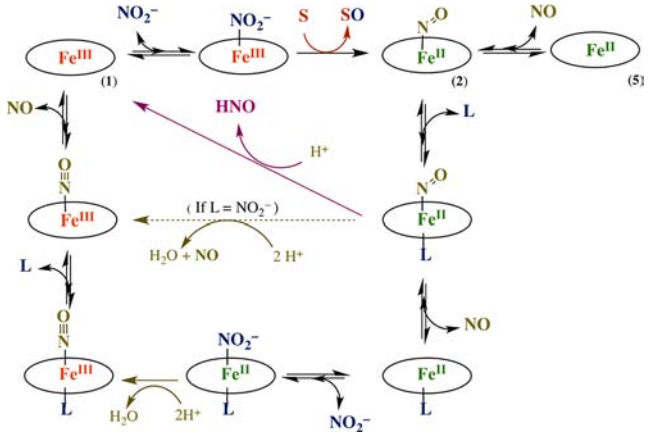

[a]Coordination sites without a ligand may be occupied by H_2O.

several competing pathways described here, the exact stoichiometry of this reaction system is likely to be a subtle function of the conditions. Initial OAT from the ferric *N*-nitrito complex forms the ferrous nitrosyl **2** plus the oxidized substrate (tpptsO, DMSO, CysS(O)H, or GS(O)H, respectively). For S = CysSH or GSH, the sulfenic acid initially formed reacts rapidly with the excess RSH to form the corresponding disulfide, RSSR (Scheme 2, $k > 720$ M^{-1} s^{-1}).[60] In addition, we

dx.doi.org/10.1021/ja312092x | J. Am. Chem. Soc. 2013, 135, 4007−4017

show that in these weakly acidic media (pH ≈ 6) the ferrous nitrosyl is simply not as inert as commonly assumed. One decay process is the slow formation of HNO, presumably by protonation of the metal nitrosyl, because this pathway is quite pH dependent.[61] Another involves the nitrite reduction by ferrous complex(es) via rate-limiting NO dissociation from the ferrousnitrosyl promoted by various proximal ligands. By analogy, the bacterial nitrite reductase *P. aeruginosa* c,d_1 NIR and wild-type cytochrome P_{450} BM3 have nitric oxide off rates that are $>10^3$ times faster than most Fe(II) nitrosyls.[62,63] Computational studies suggest that NO loss may be facilitated by direct reaction of NO_2^- with **2** to give a ferrous nitrosyl *N*-nitrito complex $Fe^{II}(TPPS)(NO)(NO_2^-)$. It is likely that the proximal ligand also plays a role in activating the ferrous coordinated NO toward protonation and release of HNO.

Endogenous formation of HNO has been speculated for many years.[47] The difficulty in detecting this elusive species is due to its inherent reactivity and the dependence on indirect markers for HNO. Nitric oxide synthase (NOS) has been considered to be a likely candidate for HNO production, and various mechanisms have been proposed.[64−68] Fukuto et al. have shown that N^{ω}-hydroxy-L-arginine (L-NOHA, a reaction intermediate during NOS turnover) can be uncoupled from NOS and subsequently oxidized to form HNO.[65] Another mechanism depends on the bioavailability of the NOS cofactor tetrahydrobiopterin (BH_4), which was shown to be necessary for production of NO. During turnover conditions without BH_4, the ferrous nitrosyl ($Fe^{II}NO$) complex of NOS accumulates and HNO is formed.[67] The exact sequence for HNO (NO^-) or $Fe^{II}NO$ formation has not been determined; however, an essential comparison of NOS turnover to our system is that after formation of the ferrous nitrosyl (the so-called "futile pathway"),[69] HNO formation is continuous until the resting ferric state is reached.

Although the present studies were carried out at pH values lower than considered typical of tissues or circulatory fluids in mammalian physiology, it should be noted that there are various environments where a lower pH is indeed relevant. For example, the tissue of organs suffering ischemia/reperfusion injury often becomes relatively acidic,[70] and that protein expression of inducible NOS, a potential source of HNO, increases during ischemic preconditioning.[71] In this context, the types of processes described here are consistent with the perceived protective roles of inorganic nitrite during I/R injury that have been attributed in part to NO formation.[1,2] Given that HNO has also been ascribed to protective properties,[47] the present studies may be doubly relevant with regard to the mechanisms of nitrite protection under these circumstances. Other acidic microenvironments have been documented. The pH ranges from 5.5 to 7.0 along the GI tract[72] and from 4.5 to 6.5 in the organelles involved in the removal of cellular waste (endosomes, lysosomes, phagosomes).[73] The role of NO in these environments has not been fully investigated; however, high levels of nitrite are present in acidic phagosomes to help destroy invading pathogens. In these contexts, it is interesting to hypothesize that production of NO and even HNO by pathways analogous to those described here could add to the diverse signaling mechanisms associated with nitrite biology.

■ ASSOCIATED CONTENT

Ⓢ Supporting Information

Twelve figures, one table, and two schemes. This material is available free of charge via the Internet at http://pubs.acs.org.

■ AUTHOR INFORMATION

Corresponding Author

ford@chem.ucsb.edu

Notes

The authors declare no competing financial interest.

■ ACKNOWLEDGMENTS

This work was supported by the Chemistry Division of the U.S. National Science Foundation (CHE-0749524 and CHE-1058794). J.L.H. thanks the ConvEne IGERT Program (NSF-DGE 0801627) for a fellowship, and we also thank Prof. Jon Fukuto of Sonoma State University for providing the Angeli's salt used in these studies.

■ REFERENCES

(1) (a) Shiva, S.; Gladwin, M. T. *Basic Res. Cardiol.* **2009**, *104*, 113−9. (b) Tejero, J.; Basu, S.; Helms, C.; Hogg, N.; King, S. B.; Kim-Shapiro, D. B.; Gladwin, M. T.; Low, N. O. *J. Biol. Chem.* **2012**, *287*, 18262−18274.

(2) (a) Lundberg, J.; Weitzberg, E.; Gladwin, M. T. *Nat. Rev. Drug Discovery* **2008**, *7*, 156−67. (b) Castiglione, N.; Rinaldo, S.; Giardina, G.; Stelitano, V.; Cutruzzola, F. *Antioxid. Redox Signaling* **2012**, *17*, 684−716. (c) Hines, I. N.; Grisham, M. B. *J. Clin. Biochem. Nutr.* **2011**, *48*, 50−56.

(3) However, see also: Luchsinger, B. P.; Rich, E. N.; Yan, Y.; Williams, E. M.; Stamler, J. S.; Singel, D. J. *J. Inorg. Biochem.* **2005**, *99*, 912−21.

(4) Hendgen-Cotta, U. B.; Kelm, M.; Rassaf, T. *Nitric Oxide-Biol. Chem.* **2010**, *22*, 75−82.

(5) Tsuchiya, K.; Kanematsu, Y.; Yoshizumi, M.; Ohnishi, H.; Kirima, K.; Izawa, Y.; Shikishima, M.; Ishida, T.; Kondo, S.; Kagami, S.; Takiguchi, Y.; Tamaki, T. *Am. J. Physiol.* **2005**, *288*, H2163−70.

(6) Feelisch, M.; Fernandez, B. O.; Bryan, N. S.; Garcia-Saura, M. F.; Bauer, S.; Whitlock, D. R.; Ford, P. C.; Janero, D. R.; Rodriguez, J.; Ashrafian, H. *J. Biol. Chem.* **2008**, *283*, 33927−34.

(7) Huang, K. T.; Keszler, A.; Patel, N.; Patel, R. P.; Gladwin, M. T.; Kim-Shapiro, D. B.; Hogg, N. *J. Biol. Chem.* **2005**, *280*, 31126−31.

(8) Nagababu, E.; Ramasamy, S.; Abernethy, D. R.; Rifkind, J. M. *J. Biol. Chem.* **2003**, *278*, 46349−56.

(9) Shiva, S.; Huang, Z.; Grubina, R.; Sun, J.; Ringwood, L. A.; MacArthur, P. H.; Xu, X.; Murphy, E.; Darley-Usmar, V. M.; Gladwin, M. T. *Circ. Res.* **2007**, *100*, 654−61.

(10) Yi, J.; Heinecke, J.; Tan, H.; Ford, P. C.; Richter-Addo, G. B. *J. Am. Chem. Soc.* **2009**, *131*, 18119−28.

(11) Heinecke, J.; Yi, J.; Pereira, J. C. M.; Richter-Addo, G. B.; Ford, P. C. *J. Inorg. Biochem.* **2012**, *107*, 47−53.

(12) Tiso, M.; Tejero, J.; Basu, S.; Azarov, I.; Wang, X.; Simplaceanu, V.; Frizzell, S.; Jayaraman, T.; Geary, L.; Shapiro, C.; Ho, C.; Shiva, S.; Kim-Shapiro, D. B.; Gladwin, M. T. *J. Biol. Chem.* **2011**, *286*, 18277−89.

(13) Webb, A. J.; Milsom, A. B.; Rathod, K. S.; Chu, W. L.; Qureshi, S.; Lovell, M. J.; Lecomte, F. M. J.; Perrett, D.; Raimondo, C.; Khoshbin, E.; Ahmed, Z.; Uppal, R.; Benjamin, N.; Hobbs, A. J.; Ahluwalia, A. *Circ. Res.* **2008**, *103*, 957−964.

(14) Heinecke, J.; Ford, P. C. *Coord. Chem. Rev.* **2010**, *254*, 235−247.

(15) Rose, E. J.; Hoffman, B. M. *J. Am. Chem. Soc.* **1983**, *105*, 2866−73.

(16) Laverman, L. E.; Ford, P. C. *J. Am. Chem. Soc.* **2001**, *123*, 11614−22.

(17) Ford, P. C.; Laverman, L. E.; Lorkovic, I. M. *Adv. Inorg. Chem.* **2003**, *51*, 203−257.

(18) Doyle, M. P.; Hoekstra, J. W. *J. Inorg. Biochem.* **1981**, *14*, 351−8.

(19) Olson, J. S.; Foley, E. W.; Rogge, C.; Tsai, A. L.; Doyle, M. P.; Lemon, D. D. *Free Radical Biol. Med.* **2004**, *36*, 685−697.

(20) Shiva, S.; Rassaf, T.; Patel, R. P.; Gladwin, M. T. *Cardiovasc. Res.* **2011**, *89*, 566−573.

(21) Tovrog, B. S.; Diamond, S. E.; Mares, F. *J. Am. Chem. Soc.* **1979**, *101*, 270−272.
(22) Ercolani, C.; Paoletti, A. M.; Pennesi, G.; Rossi, G. *J. Chem. Soc., Dalton Trans.* **1991**, 1317−1321.
(23) O'Shea, S. K.; Wang, W.; Wade, R. S.; Castro, C. E. *J. Org. Chem.* **1996**, *61*, 6388−6395.
(24) Cheng, L.; Powell, D. R.; Khan, M. A.; Richter-Addo, G. B. *Chem. Commun.* **2000**, 2301−2302.
(25) Kurtikyan, T. S.; Hovhannisyan, A. A.; Iretskii, A. V.; Ford, P. C. *Inorg. Chem.* **2009**, *48*, 11236−11241.
(26) (a) Treinin, A.; Hayon, E. *J. Am. Chem. Soc.* **1970**, *92*, 5821−8. (b) Markovits, G. Y.; Schwartz, S. E.; Newman, L. *Inorg. Chem.* **1981**, *20*, 445−450. (c) Williams, D. L. H. *Nitrosation Reactions and the Chemistry of Nitric Oxide*; Elsevier: Amsterdam, 2004.
(27) Bard, A. J., Parsons, R., Jordan, J., Eds. *Standard Potentials in Aqueous Solutions*; Marcel Dekker: New York, 1985; pp 127−139.
(28) Khin, C. Ph.D Dissertation, University of California, Santa Barbara, CA, 2008.
(29) TPPS is tetrakis(4-sulfonatophenyl)-porphyrinato, Fe^{III}(TPPS) = $Fe^{III}(TPPS)(H_2O)_2^{3-}$ (Na^+ salt). TMPS is tetrakis(sulfonatomesityl)porphyrinato, Fe^{III}(TMPS) = $Fe^{III}(TMPS)(H_2O)_2^{3-}$ (Na^+ salt). TPP is tetraphenylporphyrinato.
(30) Khin, C.; Heinecke, J.; Ford, P. C. *J. Am. Chem. Soc.* **2008**, *130*, 13830−13831 and supporting information.
(31) Heinecke, J.; Ford, P. C. *J. Am. Chem. Soc.* **2010**, *132*, 9240−9243 and supporting information.
(32) Ford, P. C. *Inorg. Chem.* **2010**, *49*, 6226−6239.
(33) Bartik, T.; Bartik, B.; Hanson, B. E.; Glass, T.; Bebout, W. *Inorg. Chem.* **1992**, *31*, 2667−2670.
(34) Lim, M. D.; Lorkovic, I. M.; Ford, P. C. *Methods Enzymol.* **2005**, *396*, 3−17.
(35) Shaw, A. W.; Vosper, A. J. *J. Chem. Soc., Faraday Trans. 1* **1977**, *73*, 1239−1244.
(36) Wilhelm, E.; Battino, R.; Wilcock, R. J. *Chem. Rev.* **1977**, *77*, 219−262.
(37) Suarez, S .A.; Fonticelli, M. H.; Rubert, A. A.; de la Llave, E.; Scherlis, D.; Salvarezza, R. C.; Martí, M. A.; Doctorovich, F. A. *Inorg. Chem.* **2010**, *49*, 6955−6966.
(38) (a) Hoshino, M.; Maeda, M.; Konishi, R.; Seki, H.; Ford, P. C. *J. Am. Chem. Soc.* **1996**, *118*, 5702−5707. (b) Fernandez, B. O.; Lorkovic, I. M.; Ford, P. C. *Inorg. Chem.* **2004**, *43*, 5393−5402.
(39) Conradie, J.; Ghosh, A. *Inorg. Chem.* **2006**, *45*, 4902−4909.
(40) Allison, W. S. *Acc. Chem. Res.* **1976**, *9*, 293−299.
(41) (a) Percival, M. D.; Ouellet, M.; Campagnolo, C.; Claveau, D.; Li, C. *Biochemistry* **1999**, *38*, 13574−13583. (b) Poole, L. B.; Zeng, B. B.; Knaggs, S. A.; Yakubu, M.; King, S. B. *Bioconjugate Chem.* **2005**, *16*, 1624−1628.
(42) Rimmer, R. D.; Richter, H.; Ford, P. C. *Inorg. Chem.* **2009**, *49*, 1180−5.
(43) Shafirovich, V.; Lymar, S. V. *Proc. Natl. Acad. Sci. U.S.A.* **2002**, *99*, 7340−5.
(44) Doyle, M. P.; Mahapatro, S. N.; Broene, R. D.; Guy, J. K. *J. Am. Chem. Soc.* **1988**, *110*, 593−599.
(45) Wong, P. S.-Y.; Hyun, J.; Fukuto, J. M.; Shirota, F. N.; DeMaster, E. G.; Shoeman, D. W.; Nagasawa, H. T. *Biochemistry* **1998**, *37*, 5362−5371 [erratum, p 18129].
(46) Shoeman, D. W.; Shirota, F. N.; DeMaster, E. G.; Nagasawa, H. T. *Alcohol* **2000**, *20*, 55−59.
(47) Miranda, K. M. *Coord. Chem. Rev.* **2005**, *249*, 433−455.
(48) (a) Reisz, J. A.; Klorig, E. B.; Wright, M. W.; King, S. B. *Org. Lett.* **2009**, *11*, 2719−21. (b) Reisz, J. A.; Zink, C. N.; King, S. B. *J. Am. Chem. Soc.* **2011**, *133*, 11675−11680.
(49) Lymar, S. V.; Shafirovich, V.; Poskrebyshev, G. A. *Inorg. Chem.* **2005**, *44*, 5212−5221.
(50) Lim, M. D.; Lorkovic, I. M.; Ford, P. C. *Inorg. Chem.* **2002**, *41*, 1026−28.
(51) Hine, J. *Physical Organic Chemistry*; McGraw-Hill Book Co.: New York, 1962; p 87.
(52) Zhao, Y.-L.; Bartberger, M. D.; Goto, K.; Shimada, K.; Kawashima, T.; Houk, K. N. *J. Am. Chem. Soc.* **2005**, *127*, 7964−7965.
(53) A recent study (ref 54) of the analogous NO oxidation of a monosulfonated triphenylphosphine in acidic solution (2−5 mM H^+) gave a larger k_9 value (5.2×10^6 M^{-2} s^{-1} at 298 K). The difference between this rate constant and that described here for tppts in pH 5.81 solution led us to conduct an independent reinvestigation of the latter system. Kinetics studies with 25 μM tppts and 0.25−0.93 mM NO confirmed the $k_9[NO]^2$[tppts] form of the rate law for tppts oxidation, with $k_9 = (3.9 \pm 0.3) \times 10^4$ M^{-2} s^{-1} at pH 5.8 and $(3.7 \pm 0.4) \times 10^4$ M^{-2} s^{-1} at pH 3.0. These values are in good agreement with the k_9 described in the text and indicate no pH effect on the reaction rate.
(54) Bakac, A.; Schouten, M.; Johnson, A.; Song, W.; Pestovsky, O.; Szajna-Fuller, E. *Inorg. Chem.* **2009**, *48*, 6979−6985.
(55) Kharitonove, V. G.; Sundquist, A. R.; Sharma, V. S. *J. Biol. Chem.* **1995**, *270*, 28158−28164.
(56) It should be noted that the design of the Schlenk cell, which has a sizable gas phase volume, provides a very large sink for any gases generated during a reaction. This is especially the case for NO given the partition coefficient favoring the gas phase over the aqueous phase.
(57) Dithionite could not be removed by chromatography due to the tendency of Fe^{II}(TPPS) to stick on a G-25 Sephadex column; therefore, the reactions were started 15 min after complete decomposition of dithionite (λ_{max} 314 nm (8000 M^{-1} cm^{-1}) (ref 56b)). Holman, D. A.; Bennett, D. W. *J. Phys. Chem.* **1994**, *98*, 13300−7.
(58) Goodrich, L. E.; Paulat, F.; Praneeth, V. K. K.; Lehnert, N. *Inorg. Chem.* **2010**, *49*, 6293−6316.
(59) (a) Paulsen, C. E.; Carroll, K. S. *ACS Chem. Biol.* **2010**, *5*, 47−62. (b) Roos, G.; Messens, J. *Free Radical Biol. Med.* **2011**, *51*, 314−326. (c) Vazquez-Torres, A. *Antioxid. Redox Signaling* **2012**, *17*, 1201−1214.
(60) (a) Claiborne, A.; Miller, H.; Parsonage, D.; Ross, R. P. *FASEB J.* **1993**, *7*, 1483−1490. (b) Ashby, M. T.; Nagy, P. *J. Pharm. Sci.* **2006**, *95*, 15−18.
(61) (a) Note that this reaction is reversible given that ferriheme models and proteins are known to react with HNO to give the analogous ferroheme nitrosyls (refs 61b and 61c). (b) Miranda, K. M.; Nims, R. W.; Thomas, D. D.; Espey, M. G.; Citrin, D.; Bartberger, M. D.; Paolocci, N.; Fukuto, J. M.; Feelisch, M.; Wink, D. A. *J. Inorg. Biochem.* **2003**, *93*, 52−60. (c) Suárez, S. A.; Martí, M. A.; De Biase, P. M.; Estrin, D. A.; Bari, S. E.; Doctorovich, F. *Polyhedron* **2007**, *26*, 4673−4679.
(62) Rinaldo, S.; Arcovito, A.; Brunori, M.; Cutruzzola, F. *J. Biol. Chem.* **2007**, *282*, 14761−14767.
(63) Quaroni, L. G.; Seward, H. E.; McLean, K. J.; Girvan, H. M.; Ost, T. W. B.; Noble, M. A.; Kelly, S. M.; Price, N. C.; Cheesman, M. R.; Smith, W. E.; Munro, A. W. *Biochemistry* **2004**, *43*, 16416−16431.
(64) Schmidt, H. H. W.; Hofmann, H.; Schindle, R. U.; Shutenko, Z. S.; Cunningham, D. D.; Feelisch, M. *Proc. Natl. Acad. Sci. U.S.A.* **1996**, *93*, 14492−14497.
(65) Fukuto, J. M.; Wallace, G. C.; Hszieh, R.; Chaudhuri, G. *Biochem. Pharmacol.* **1992**, *43*, 607−613.
(66) Pufahl, R. A.; Wishnok, J. S.; Marletta, M. A. *Biochemistry* **1995**, *3*, 1930−1941.
(67) Adak, S.; Wang, Q.; Stuehr, D. J. *J. Biol. Chem.* **2000**, *275*, 33554−33561.
(68) Fukuto, J. M.; Stuehr, D. J.; Feldman, P. L.; Bova, M. P.; Wong, P. *J. Med. Chem.* **1993**, *36*, 2666−2670.
(69) Santolini, J.; Meade, A. L.; Stuehr, D. J. *J. Biol. Chem.* **2001**, *276*, 48887−48898.
(70) Zweier, J. L.; Samouilov, A.; Kuppusamy, P. *Biochim. Biophys. Acta, Bioenerg.* **1999**, *1411*, 250−262.
(71) Wang, Y.; Guo, Y.; Zhang, S. X.; Wu, W.; Wang, J.; Bao, W.; Bolli, R. *J. Mol. Cell Cardiol.* **2002**, *34*, 5−15.
(72) Nugent, S. G.; Kumar, D. *Gut* **2001**, *48*, 571−577.
(73) (a) Sorkin, A.; von Zastrow, M. *Nat. Rev. Mol. Cell Biol.* **2002**, *3*, 600−614. (b) Geisow, M. J.; Hart, P. D.; Young, M. R. *J. Cell Biol.* **1981**, *89*, 645−652.